Tumor suppressor function of miR-483-3p on breast cancer via targeting of the cyclin E1 gene

XIAOXI HUANG[1*] and JIN LYU[2*]

[1]Department of Breast, Fujian Provincial Maternity and Children Hospital of Fujian Medical University, Fuzhou, Fujian 350001; [2]Department of Surgical Oncology, Nanjing First Hospital, Nanjing Medical University, Nanjing, Jiangsu 210006, P.R. China

Received June 14, 2017; Accepted November 3, 2017

DOI: 10.3892/etm.2018.6504

Abstract. microRNA (miR)-483-3p has previously been demonstrated to be a tumor suppressor in many types of cancer cells, however it is unknown whether miR-483-3p is involved in the regulation of breast cancer. Therefore, the aim of the present study was to investigate the effects of miR-483-3p on breast cancer. The results demonstrated that the expression of miR-483-3p was decreased, especially in MCF-7 cells. The results of CCK-8 assay and cell cycle analysis demonstrated that miR-483-3p significantly reduced cell proliferation and inhibited MCF-7 cells in the G1 phase from entering the S phase ($P<0.01$). It was also demonstrated that Cyclin E1 (CCNE1) is a target gene of miR-483-3p using bioinformatics and a dual luciferase reporter assay. miR-483-3p inhibited the expression of CCNE1, cyclin-dependent kinase 2, nuclear protein ataxia-telangiectasia (NPAT) and phosphorylated NPAT. Therefore, the results indicated that miR-483-3p functions as a tumor suppression in breast cancer and CCNE1 is its target gene. Downstream genes of CCNE1 were also repressed by miR-483-3p. Therefore, these findings suggest that miR-483-3p is a key factor in breast cancer.

Introduction

Breast cancer is one of the most prevalent malignant tumors in females. It typically occurs between the ages of 40 and 60 years and has a high prevalence in females prior to and following the menopause (1). In 2016, breast cancer accounted for 29% of cancer diagnoses in females and became the leading cause of female associated mortality in females in the United States (2,3). The causes of breast cancer are complex (4), therefore it is necessary to identify a novel treatment strategy.

Cyclin E1 (CCNE1) gene is a member of the highly conserved cyclin family. It encodes G1/S-specific cyclin-E1 protein and is a positive regulator in the cell cycle (5). The overexpression of CCNE1 in tumors may contribute to tumorigenesis (6,7). CCNE1 is critical in ovarian cancer tumor growth and proliferation (6). Additionally, it is a novel translocation partner of the immunoglobulin heavy chain locus and a novel oncogene in B cell lymphomagenesis (8). CCNE1 was first implicated in breast cancer (9,10). The abnormal expression of CCNE1 is associated with high proliferation rates, particularly in the estrogen receptor-phenotype in breast cancer (11). Stratified analysis has previously indicated that CCNE1 may be a factor and molecular marker for breast cancer and survival in the Chinese Han population (11).

It has been demonstrated previously that microRNAs (miRNAs or miRs) serve a role in the regulation of CCNE1. miR-15a has been identified as an anti-tumor miRNA in breast cancer via targeting of CCNE1 (5). In addition, the human hepatocellular carcinoma cell cycle was arrested at G1 to S transition by miR-7 and similarly, CCNE1 was identified as its target gene (12). miR-16-1 also serves a vital role in the regulation of cell cycle processes and downregulates the expression of CCNE1 in cervical cancer (13). The present study aimed to investigate the effects of miR-483-3p on cell growth, apoptosis, migration, invasion and the cell cycle in breast cancer via targeting CCNE1.

Materials and methods

Cell culture and transfection. Three breast cancer cell lines, MCF-7, T47D, MDA-MB-231 and normal breast cell line MCF-10A (America Type Culture Collection, Manassas, VA, USA), were incubated with RPMI-1640 (Gibco; Thermo Fisher Scientific, Inc., Waltham, MA, USA) containing 10% fetal bovine serum (FBS; Thermo Fisher Scientific, Inc.), in an atmosphere of 5% CO_2 at 37˚C. Cells were then seeded in 6-well plates ($5x10^5$ cells/well) at a cell density of 70-90% and transfected using Lipofectamine® 3000 reagent (Thermo Fisher Scientific, Inc.) and 50 nM mature miR-483-3p mimics (UCACUCCUCUCCUCCCGUCUU; Guangzhou RiboBio

Correspondence to: Dr Jin Lyu, Department of Surgical Oncology, Nanjing First Hospital, Nanjing Medical University, 68 Changle Road, Nanjing, Jiangsu 210006, P.R. China
E-mail: lvjinnj@hotmail.com

*Contributed equally

Key words: microRNA-483-3p, breast cancer, cyclin E1, proliferation, cell cycle

Co., Ltd., Guangzhou, China) for 48 h according to the manufacturer's protocols. A non-homologous miRNA mimics control (cat. no. miR01201-1-5; Guangzhou RiboBio Co., Ltd.) was used as a negative control.

RNA isolation and reverse transcription-quantitative polymerase chain reaction (RT-qPCR). T47D, MDA-MB-231, MCF-7 and MCF-10A cells were cultured in 6 well plates ($5x10^5$ cells/well) and total RNA was isolated using a High Purity Total RNA Extraction kit (Bioteke Corporation, Beijing, China). Total RNA was then reverse-transcribed into cDNA using a PrimeScript RT Master Mix (Takara Biotechnology Co., Ltd., Dalian, China) according to the manufacturer's protocol. qPCR was performed at 95˚C for an initial 10 min, followed by 40 cycles of denaturation at 95˚C for 30 sec, annealing at 55˚C for 30 sec and extension at 72˚C for 30 sec using SYBR Premix Ex Taq (Takara Biotechnology Co., Ltd.). mRNA relative expression levels were calculated using the $2^{-\Delta\Delta Cq}$ method (14). GAPDH was used as the endogenous control for calculating the gene expression and U6 was used as a control for microRNA expression. The primers used for qPCR are presented in Table I. The expression of miR-483-3p was the lowest in MCF-7 cells. Thus subsequent experiments were only performed on MCF-7 cells.

Western blot analysis. Total protein was extracted from MCF-7 cells ($1x10^7$) using radioimmunoprecipitation buffer containing 1% phenylmethane sulfonyl fluoride protease inhibitor (Beyotime Institute of Biotechnology, Haimen, China). A BCA Protein assay kit was then used to determine protein concentration. Proteins (30 μg/lane) were separated by 10% SDS-PAGE and transferred to a polyvinylidene difluoride membrane (EMD Millipore, Billerica, MA, USA). The membrane was then blocked with 3% bovine serum albumin (Biosharp, Shanghai, China) at room temperature for 2 h and incubated with primary antibodies against CCNE1 (1:500; cat no. ab3927), cyclin-dependent kinase 2 (CDK2; 1:1,000; cat no. ab32147), nuclear protein ataxia-telangiectasia (NPAT; 1:1,000; cat no. ab70595), phosphorylated (p)-NPAT (1:1,000; cat no. ab70595) and GAPDH (1:5,000; cat no. ab8245; all Abcam, Cambridge, UK) overnight at 4˚C. Following washing with 1X Tween20 in Tris buffered solution three times, samples were incubated with a goat anti-mouse horseradish peroxide (HRP)-conjugated secondary antibody (1:5,000; cat no. ab205719) or goat anti-rabbit HRP-conjugated secondary antibody (1:5,000; cat no. ab205718; both Abcam) at room temperature for 2 h. The membrane was visualized using an enhanced chemiluminescence kit (Beyotime Institute of Biotechnology, Haimen, China).

Cell proliferation assay. MCF-7 cells ($1x10^5$) were seeded in a 96-well plate and cultured at 37˚C with 5% CO_2 and transfected with miRNA mimics or negative controls. A cell counting kit (CCK)-8 kit (Sigma-Aldrich; Merck KGaA, Darmstadt, Germany) was subsequently used to measure cell proliferation. Briefly, following transfection and incubation at 37˚C for 24 h, 10 μl CCK-8 solution was added to each well of the plate. Following 4 h incubation, absorbance was measured at a wavelength of 450 nm using a microplate reader.

Wound healing assay. The migration ability of MCF-7 cells was detected using a wound healing assay. MCF-7 cells ($5x10^5$/well) were seeded in 6-well dishes. Following transient transfection, cells were incubated for 12 h in a humidified incubator at 37˚C with 5% CO_2. A 'wound' was created in each culture using a sterilized 1 ml pipette. The debris was washed with PBS and cells were incubated with serum-free RPMI-1640 medium at 37˚C for 48 h. The cell migration area was quantified by observing images taken under a light microscope (Olympus Corporation, Tokyo, Japan) at a magnification of x100. Images were analyzed by ImageJ software (version 1.48; National Institutes of Health, Bethesda, MD, USA). Migration was quantified by counting the cell numbers from five fields in the wound area. Experiments were carried out in triplicate, at least three times.

Migration assay. MCF-7 cell migration was investigated using 24-well plates. Briefly, following transfection, $2.5x10^5$ cells were resuspended and incubated in RPMI-1640 medium without serum and seeded in the upper chamber of a Transwell insert at 37˚C for 48 h. RPMI 1640 containing FBS medium was added to the lower chamber. Cells were fixed using 4% paraformaldehyde at room temperature for 30 min and stained using 0.1% crystal violet (Sigma-Aldrich; Merck KGaA) at room temperature for 20 min. The migratory status of MCF-7 cells was observed under a light microscope at a magnification of x200 and assessed by the relative number of migrated cells.

Bioinformatics, vector construction and dual luciferase reporter assay. The sequence of CCNE1 3'-untranslated region (UTR) was predicted to interact with miR-483-3p using TargetScan (www.targetscan.org/vert_71/). The fragments of CCNE1, containing a wild-type 3'UTR (CCAACAUGGUGA AACCCCGUCUC) or mutated (CCAACAUGGUGAAAC *UUUAG*CUC), were inserted into the psiCHECK™-2 vector (Promega Corporation, Madison, WI, USA). Then MCF-7 cells were transfected using Lipofectamine® 3,000 reagent (Thermo Fisher Scientific, Inc.) according to the manufacturer's protocols. Following 24 h incubation of MCF-7 cells in RPMI-1640 medium at 37˚C, luciferase activity was measured using the Dual-Glo luciferase assay system (Promega Corporation). *Renilla* luciferase activity served as the internal control.

Cell cycle assay. Following transfection, MCF-7 cells were harvested when they reached 80% confluence and fixed with 70% ice-cold ethanol at 4˚C for 1 h. Cells were washed with PBS and stained with 0.1% (m/v) propidium iodide (BD Biosciences, Franklin Lakes, NJ, USA) in the dark at room temperature for 1 h. The cell cycle was analyzed by flow cytometry using a FACSCalibur flow cytometer (BD Biosciences). The percentages of cells in the G0/G1, S and G2/M phases were then determined by FlowJo software (version 7.6.1; FlowJo LLC, Ashland, OR, USA).

Statistical analysis. Data are expressed as the mean ± standard error of the mean and experiments were repeated in triplicate. Statistical differences were identified using Student's t-test or one-way analysis of variance followed by the Dunnett's t-test. Statistical analysis was performed using SPSS 20.0 (IBM

Table I. Primer sequences.

Gene	Forward (5'-3')	Reverse (5'-3')
CCNE1	TTCTTGAGCAACACCCTCTTCTGCAGCC	TCGCCATATACCGGTCAAAGAAATCTTGTGCC
CDK2	CTGCTTCCTGTTGGCTCTTTCT	CTTTGTTTCTGCCTTCTCTCCT
NPAT	TACACAGGTTACTCGACCAAGT	GCGTCTACCGGGAGACATTAAA
U6	CTCGCTTCGGCAGCACA	AACGCTTCACGAATTTGCGT
miR-483-3p	ACACTCCAGCTGGGTCACTCCTCTCCTCC	TGGTGTCGTGGAGTCG
GAPDH	GCACCGTCAAGGCTGAGAAC	TGGTGAAGACGCCAGTGGA

CCNE1, cyclin E1; CDK2, cyclin-dependent kinase 2; NPAT, nuclear protein ataxia-telangiectasia; miR-483-3p, microRNA-483-3p.

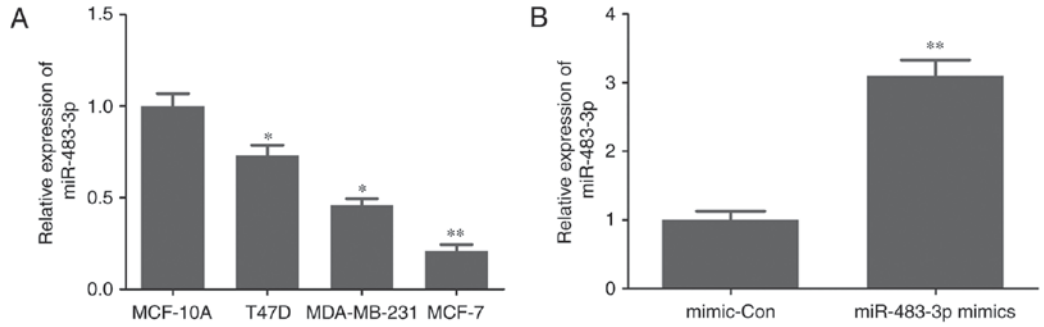

Figure 1. Expression of miR-483-3p in non-malignant breast epithelial cells and breast cancer cells. (A) miR-483-3p was downregulated in breast cancer cell lines T47D, MDA-MB-231 and MCF-7 compared with MCF-10A cells. Data are expressed as the mean ± standard error of the mean and experiments were repeated in triplicate. *P<0.05, **P<0.01 vs. MCF-10A cells. (B) Reverse transcription-quantitative polymerase chain reaction indicated that miR-483-3p was upregulated in MCF-7 cells transfected with miR-483-3p mimics. Data are expressed as the mean ± standard error of the mean and experiments were repeated in triplicate. **P<0.01 vs. the mimic-con group. miR-483-3p, microRNA-483-3p; mimic-con, mimic-control group.

Corp., Armonk, NY, USA). P<0.05 was considered to indicate a statistically significant difference.

Results

miR-483-3p is downregulated in breast cancer cells. RT-qPCR was performed to determine the level of miR-483-3p expression in normal breast cell and breast cancer cells. The expression of miR-483-3p was significantly reduced in T47D, MDA-MB-231 and MCF-7 breast cancer cells compared with MCF-10A normal breast cells (Fig. 1A). These results suggest that miR-483-3p may serve a role in breast cancer progression.

miR-483-3p decreases MCF-7 cell proliferation. The effect of miR-483-3p on cell proliferation in breast cancer was investigated by transfecting MCF-7 cells with miR-483-3p mimics (Fig. 1B). The results of the CCK-8 assay indicated that overexpression of miR-483-3p significantly inhibited cell proliferation compared with the mimic control group (Fig. 2). In addition, the cell cycle assay demonstrated that overexpression of miR-483-3p significantly retained MCF-7 cells in the G1 phase, preventing them from entering the S phase (Fig. 3). These results suggest that miR-483-3p regulates MCF-7 cell proliferation.

miR-483-3p downregulates the expression of CCNE1, CDK2, NPAT and p-NPAT. RT-qPCR and western blotting were used to measure the expression of CCNE1, CDK2 and p-NPAT following transfection, to further analyze the regulation of the cell cycle by miR-483-3p in MCF-7 cells. The results of RT-qPCR demonstrated that miR-483-3p overexpression significantly downregulated the expression of CCNE1, CDK2 and NPAT mRNA compared with that in the mimic control group (Fig. 4A-C). The results of western blotting also suggested that miR-483-3p overexpression markedly downregulated the expression of CCNE1, CDK2, NPAT and p-NPAT protein compared with the mimic control group

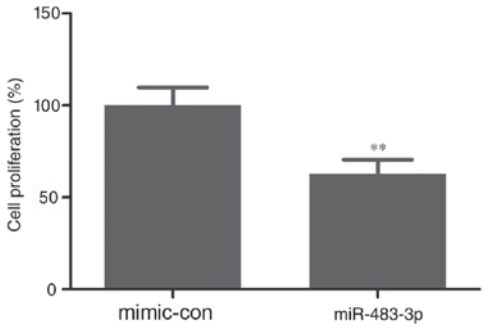

Figure 2. Cell proliferation in MCF-7 cells following transfection with miR-483-3p mimics. Overexpression of miR-483-3p suppresses MCF-7 cell proliferation in cells transfected with miR-483-3p mimics. Data are expressed as the mean ± standard error of the mean and experiments were repeated in triplicate. **P<0.01 vs. the mimic-con group. miR-483-3p, microRNA-483-3p; mimic-con, mimic-control group.

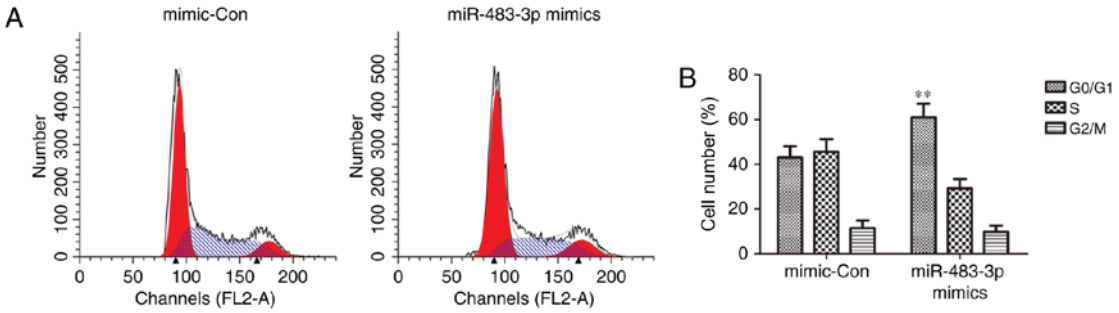

Figure 3. Overexpression of miR-483-3p inhibits MCF-7 cells in the G1 phase from progressing to the S phase. (A) Cell cycle was analyzed using flow cytometry. (B) Percentage of cells in the G0/G1, S, and G2/M phases. Data are expressed as the mean ± standard error of the mean and experiments were repeated in triplicate. **P<0.01 vs. mimic-con G0/G1 phase. miR-483-3p, microRNA-483-3p; mimic-con, mimic-control group.

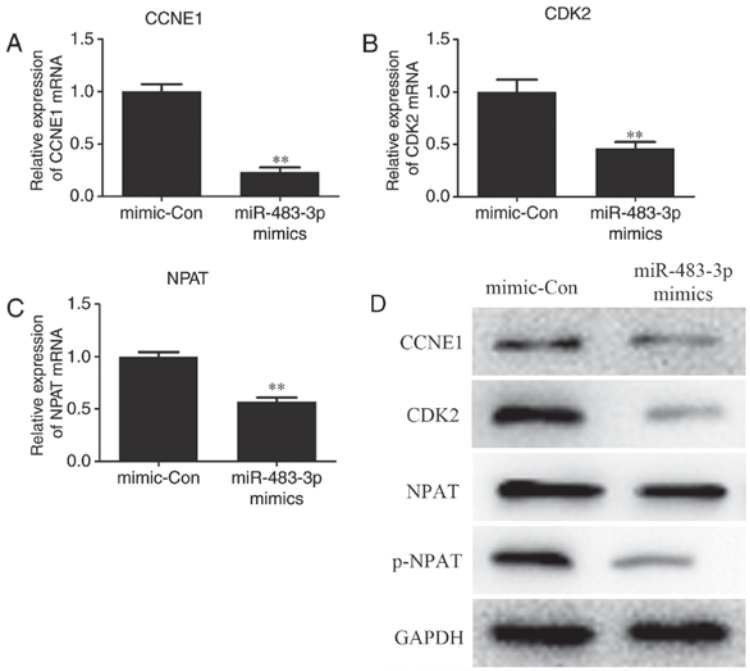

Figure 4. Overexpression of miR-483-3p inhibits the expression of CCNE1, CDK2, and NPAT mRNA and protein. MCF-7 cells were transfected with miR-483-3p mimics. The expression of (A) CCNE1 (B) CDK2 and (C) NPAT mRNA was measured using reverse transcription-quantitative polymerase chain reaction. (D) The expression of CCNE1, CDK2, NPAT and p-NPAT protein was measured using western blotting. Data are expressed as the mean ± standard error of the mean and experiments were repeated in triplicate. **P<0.01 vs. the mimic-con group. miR-483-3p, microRNA-483-3p; CCNE1, cyclin E1; CDK2, cyclin-dependent kinase 2; NPAT, nuclear protein ataxia-telangiectasia; p, phosphorylated mimic-con, mimic-control group.

(Fig. 4). These results, therefore indicated that miR-483-3p suppressed MCF-7 cell proliferation.

miR-483-3p inhibits the migration ability of MCF-7 cells. The role of miR-483-3p in the migration of breast cancer cells was demonstrated using wound healing and Transwell assays to observe the migration of MCF-7 cells following transfection. miR-483-3p overexpression significantly inhibited the wound healing ability of MCF-7 cells compared with the mimic control group (Fig. 5A and B). In addition, miR-483-3p overexpression also significantly reduced the migration ability of MCF-7 cells compared with the mimic control group (Fig. 5C and D). These findings indicated that miR-483-3p attenuates the migration ability of MCF-7 cells.

CCNE1 is the target of miR-483-3p. The molecular mechanism of miR-483-3p in regulating cell proliferation was determined by predicting the targets of miR-483-3p using TargetScan. The results indicated that CCNE1 was a target of miR-483-3p (Fig. 6A). A dual luciferase reporter assay demonstrated that miR-483-3p overexpression significantly reduced dual-luciferase activity in the wild type group compared with the mutant group (Fig. 6B). These results therefore confirmed that CCNE1 is a target of miR-483-3p.

Discussion

The role of miRs as tumor suppressors targeting molecules and signaling pathways in breast cancer, including the lethal-7, miR-125, miR-200, miR-205 and miR-206 families, has been previously suggested (15). miR-483-3p has also been reported to be associated with breast cancer and may be a featured biomarker in breast cancer when using an miRNA microarray (16).

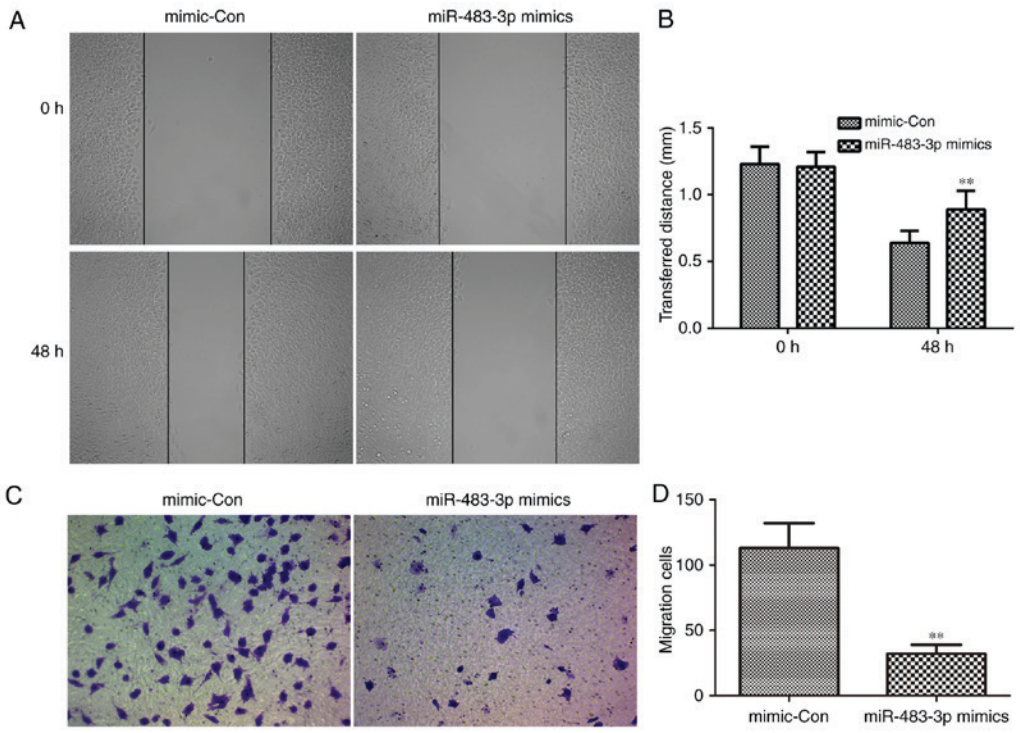

Figure 5. Overexpression of miR-483-3p decreases the migration ability of MCF-7 cells transfected with miR-483-3p mimics. (A) Images of wound healing assay (magnification, x100) and (B) quantification of the wound healing assay. (C) Images of the Transwell assay (magnification, x200) and (D) quantification of the Transwell assay. **P<0.01 vs. the mimic-con group. Data are expressed as the mean ± standard error of the mean and experiments were repeated in triplicate. miR-483-3p, microRNA-483-3p; mimic-con, mimic-control group.

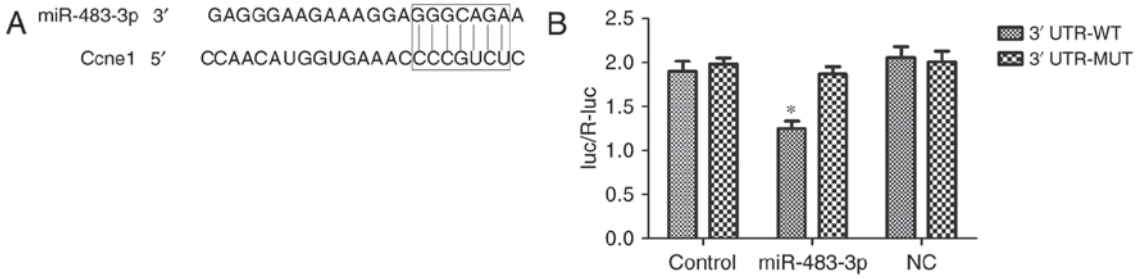

Figure 6. CCNE1 is the target gene of miR-483-3p. (A) Predicted WT miR-483-3p binding sites at the 3'-UTR of CCNE1. (B) Dual luciferase reporter assay indicated miR-483-3p bound directly to the 3'-UTR of CCNE1. Data are expressed as the mean ± standard error of the mean and experiments were repeated in triplicate. *P<0.05 vs. 3'UTR-MUT. CCNE1, cyclin E1; miR-483-3p, microRNA-483-3p; UTR, untranslated region; R-luc, Renilla luciferase; NC, negative control; WT, wild type; MUT, mutant.

miR-483 was initially identified in the human fetal liver (16) and is located within intron 2 of the insulin-like growth factor 2 locus (17). It serves important roles in the mechanism of many diseases, including alcoholic hepatitis (18), diabetic cardiomyopathy (19), ovarian carcinoma (20) and pancreatic cancer (21). In the present study, the effect of miR-483-3p in breast cancer was investigated and the results demonstrated that miR-483-3p was downregulated in breast cancer cell lines, especially in MCF7 cells. These results suggest the potential tumor suppressor function of miR-483-3p. Therefore, MCF7 cells were transfected with miR-483-3p mimics and it was demonstrated that overexpression of miR-483-3p decreased cell proliferation and suppressed cell migration.

It was also demonstrated that miR-483-3p overexpression suppressed MCF-7 cells in the G1 phase from entering the S phase. CCNE1 forms a complex with CDK2 and CCNE1-CDK2 regulates the cell cycle, as it is a key kinase complex in G1-S transition (22). It induces cells to initiate DNA synthesis via phosphorylation of their downstream substrates, including NPAT, thereby allowing cells to irreversibly enter the S phase (23). Hence, to further investigate the effects of miR-483-3p overexpression on the cell cycle, the expression of CCNE1, CDK2 and p-NPAT protein was detected using western blot analysis. The results demonstrated that miR-483-3p overexpression markedly reduced the expression of CCNE1, CDK2 and p-NPAT protein.

Cyclin E1 is encoded by the CCNE1 gene (Gene ID: 898) and belongs to the cyclin family (11). Bioinformatics analysis predicted that the CCNE1 gene was a target gene of miR-483-3p. In addition, the results of the dual-luciferase reporter assay indicated that CCNE1 is a direct target of miR-483-3p.

In conclusion, the results of the present study indicated that miR-483-3p is a key factor in breast cancer and inhibits G1-S transition in the cell cycle of MCF-7 cells. These findings suggest that miR-483-3p has a tumor suppression role in breast cancer and CCNE1 is its direct target. Therefore, miR-483-3p may be a novel therapy for the treatment of breast cancer.

References

1. Dodiyi-Manuel A and Wakama IE: Predispositions of carcinoma of the breast: A review. Niger J Med 23: 7-12, 2014.
2. Siegel RL, Miller KD and Jemal A: Cancer statistics, 2016. CA Cancer J Clin 66: 7-30, 2016.
3. Panieri E: Breast-cancer awareness in low-income countries. Lancet Oncol 14: 274-275, 2013.
4. Zhang BN, Cao XC, Chen JY, Chen J, Fu L, Hu XC, Jiang ZF, Li HY, Liao N, Liu DG, *et al*: Guidelines on the diagnosis and treatment of breast cancer (2011 edition). Gland Surg 1: 39-61, 2012.
5. Luo Q, Li X, Li J, Kong X, Zhang J, Chen L, Huang Y and Fang L: MiR-15a is underexpressed and inhibits the cell cycle by targeting CCNE1 in breast cancer. Int J Oncol 43: 1212-1218, 2013.
6. Nakayama N, Nakayama K, Shamima Y, Ishikawa M, Katagiri A, Iida K and Miyazaki K: Gene amplification CCNE1 is related to poor survival and potential therapeutic target in ovarian cancer. Cancer 116: 2621-2634, 2010.
7. Coradini D, Boracchi P, Oriana S, Biganzoli E and Ambrogi F: Differential expression of genes involved in the epigenetic regulation of cell identity in normal human mammary cell commitment and differentiation. Chin J Cancer 33: 501-510, 2014.
8. Nagel I, Akasaka T, Klapper W, Gesk S, Böttcher S, Ritgen M, Harder L, Kneba M, Dyer MJ and Siebert R: Identification of the gene encoding cyclin E1 (CCNE1) as a novel IGH translocation partner in t(14;19)(q32;q12) in diffuse large B-cell lymphoma. Haematologica 94: 1020-1023, 2009.
9. Keyomarsi K and Pardee AB: Redundant cyclin overexpression and gene amplification in breast cancer cells. Proc Natl Acad Sci USA 90: 1112-1116, 1993.
10. Sutherland RL and Musgrove EA: Cyclins and breast cancer. J Mammary Gland Biol Neoplasia 9: 95-104, 2004.
11. Han JY, Wang H, Xie YT, Li Y, Zheng LY, Ruan Y, Song AP, Tian XX and Fang WG: Association of germline variation in CCNE1 and CDK2 with breast cancer risk, progression and survival among Chinese Han women. PLoS One 7: e49296, 2012.
12. Zhang X, Hu S, Zhang X, Wang L, Zhang X, Yan B, Zhao J, Yang A and Zhang R: MicroRNA-7 arrests cell cycle in G1 phase by directly targeting CCNE1 in human hepatocellular carcinoma cells. Biochem Biophys Res Commun 443: 1078-1084, 2014.
13. Zubillaga-Guerrero MI, Alarcon-Romero Ldel C, Illades-Aguiar B, Flores-Alfaro E, Bermúdez-Morales VH, Deas J and Peralta-Zaragoza O: MicroRNA miR-16-1 regulates CCNE1 (cyclin E1) gene expression in human cervical cancer cells. Int J Clin Exp Med 8: 15999-16006, 2015.
14. Livak KJ and Schmittgen TD: Analysis of relative gene expression data using real-time quantitative PCR and the 2(-Delta Delta C(T)) method. Methods 25: 402-408, 2001.
15. Asghari F, Haghnavaz N, Baradaran B, Hemmatzadeh M and Kazemi T: Tumor suppressor microRNAs: Targeted molecules and signaling pathways in breast cancer. Biomed Pharmacother 81: 305-317, 2016.
16. Zhang M, Liu D, Li W, Wu X, Gao C and Li X: Identification of featured biomarkers in breast cancer with microRNA microarray. Arch Gynecol Obstet 294: 1047-1053, 2016.
17. Veronese A, Lupini L, Consiglio J, Visone R, Ferracin M, Fornari F, Zanesi N, Alder H, D'Elia G, Gramantieri L, *et al*: Oncogenic role of miR-483-3p at the IGF2/483 locus. Cancer Res 70: 3140-3149, 2010.
18. Liu H, French BA, Li J, Tillman B and French SW: Altered regulation of miR-34a and miR-483-3p in alcoholic hepatitis and DDC fed mice. Exp Mol Pathol 99: 552-557, 2015.
19. Qiao Y, Zhao Y, Liu Y, Ma N, Wang C, Zou J, Liu Z, Zhou Z, Han D, He J, *et al*: miR-483-3p regulates hyperglycaemia-induced cardiomyocyte apoptosis in transgenic mice. Biochem Biophys Res Commun 477: 541-547, 2016.
20. Arrighetti N, Cossa G, De Cecco L, Stucchi S, Carenini N, Corna E, Gandellini P, Zaffaroni N, Perego P and Gatti L: PKC-alpha modulation by miR-483-3p in platinum-resistant ovarian carcinoma cells. Toxicol Appl Pharmacol 310: 9-19, 2016.
21. Hao J, Zhang S, Zhou Y, Hu X and Shao C: MicroRNA 483-3p suppresses the expression of DPC4/Smad4 in pancreatic cancer. FEBS Lett 585: 207-213, 2011.
22. Deng M, Li F, Ballif BA, Li S, Chen X, Guo L and Ye X: Identification and functional analysis of a novel cyclin e/cdk2 substrate ankrd17. J Biol Chem 284: 7875-7888, 2009.
23. Zhao J, Kennedy BK, Lawrence BD, Barbie DA, Matera AG, Fletcher JA and Harlow E: NPAT links cyclin E-Cdk2 to the regulation of replication-dependent histone gene transcription. Genes Dev 14: 2283-2297, 2000.